available at www.sciencedirect.com

ScienceDirect

journal homepage: www.elsevier.com/locate/ecolmodel

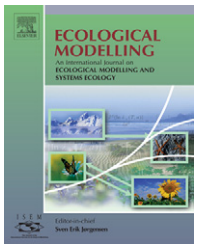

Ecosystem change in the western North Pacific associated with global warming using 3D-NEMURO

Taketo Hashioka [a,*], *Yasuhiro Yamanaka* [b,c]

[a] *Graduate School of Environmental Earth Science, Hokkaido University, N10W5, Kita-ku, Sapporo, Hokkaido 060-0810, Japan*
[b] *Graduate School of Environmental Science, Hokkaido University, N10W5, Kita-ku, Sapporo, Hokkaido 060-0810, Japan*
[c] *Global Warming Research Program, Frontier Research System for Global Change, Frontier Research Center for Global Change, 3173-25 Showamachi, Kanazawa-ku, Yokohama City, Kanagawa 236-0001, Japan*

ARTICLE INFO

Article history:
Published on line 16 November 2006

Keywords:
3D-NEMURO
Biogeochemical cycles
Climate change
Ecosystem change
Ecosystem model
Global warming
NEMURO
North Pacific

ABSTRACT

We developed a 3D ecosystem-biogeochemical model based on NEMURO (North Pacific Ecosystem Model Used for Regional Oceanography) and applied it to the western North Pacific in order to predict the effects of global warming on ecosystem dynamics and biogeochemical cycles. Using datasets of observed climatology and simulated fields according to a global warming scenario, IS92a (CO-AGCM developed by CCSR/NIES) as boundary conditions for our ecosystem model, we conducted present-day and global warming experiments and compared their results. Model results in the global warming experiment show increases in vertical stratification due to rising temperatures. As a result, the predicted nutrient and chlorophyll-*a* concentrations in the surface water decrease at the end of the 21st century, and the dominant phytoplankton group shifts from diatoms to other small phytoplankton. The P/B ratio slightly increases from that in the present as a result of favorable temperature conditions, although nutrient conditions become worse. The increase in the P/B ratio causes increases in the NPP and GPP, although new and export productions decrease. Increases in the regeneration rates (i.e., decrease in the e-ratio) also contribute to increases in NPP and GPP through nutrient supplies within the surface water. Changes in seasonal variations of biomass and the dominant phytoplankton group in the subarctic–subtropical transition region associated with the global warming are large in all regions. In the global warming scenario, the onset of the diatom spring bloom is predicted to take place 1.5 month earlier than in the present-day simulation due to strengthened stratification. The maximum biomass in the spring bloom is predicted to decrease drastically compared to the present due to the decreases in nutrient concentration. In contrast, the biomass maximum of the other small phytoplankton at the end of the diatom spring bloom is the same as the present, because they can adapt to the low nutrient conditions due to their small half-saturation constant. Therefore, a change in the dominant phytoplankton group appears notably at the end of spring bloom. Since the present nutrient concentrations and phytoplankton biomass from summer to winter are low compared with those in spring, these changes associated with the global warming are small. That is, it is interesting that the changes do not occur uniformly in all seasons, but occur dramatically at the end of the spring and in the fall bloom.

* *Corresponding author*. Tel.: +81 11 706 2374; fax: +81 11 706 4865.
E-mail address: hashioka@ees.hokudai.ac.jp (T. Hashioka).
0304-3800/$ – see front matter © 2006 Elsevier B.V. All rights reserved.
doi:10.1016/j.ecolmodel.2005.12.002

1. Introduction

Changes in the physical environment associated with the global warming (temperature, light intensity, vertical stratification and horizontal flow fields) affect ecosystem dynamics and biogeochemical cycles. We generally consider effects of global warming on photosynthetic rate through the following processes. Warming in the surface water directly affects photosynthetic rate due to its temperature dependence and indirectly affects the other conditions for photosynthesis through stratification between the surface and subsurface waters. Stratification has two effects: improvement of light conditions due to the shoaling of the mixed layer depth (MLD) and suppression of nutrient supply from the deep water associated with winter mixing. Also, since decomposition and remineralization rates of particulate organic matter increase with rising temperatures, the nutrient regeneration rates increase in the surface water. Grazing pressure by zooplankton also increases with temperature. Therefore, we must quantitatively investigate changes of each process under global warming in order to understand its effects on ecosystem dynamics.

As a general hypothesis, global warming affects the ecosystem as follows: (1) increases in temperature and rainfall will cause increased vertical stratification in the surface water, (2) nutrients supplied from the deep water will decrease due to a weakened vertical convection and (3) biological production will decrease, associated with a change in composition of the phytoplankton groups due to the decreases in nutrient supplies (e.g., diatoms as percentage of total phytoplankton will decrease and the percentage of the other non-diatom small phytoplankton, including cocolithophorids, will increase). These general hypotheses become more realistic based on recent observations of decreasing trends in nutrients and a shift to small phytoplankton groups during the last 30 years in the North Pacific (Watanabe et al., 2003, 2005). As a positive feedback to the global climate change, it is also suggested that biogeochemical cycles would change in association with the transition of phytoplankton groups and with changes in the physical environment and that the efficiency of oceanic CO_2 uptake would decrease. For example, increases in cocolithophorids, which make $CaCO_3$ shells, will cause an increase in the C_{org}:$CaCO_3$ export ratio and this increase would decrease the ocean pH and decrease oceanic capacity to take up the anthropogenic CO_2 (Archer and Maier-Reimer, 1994; Archer et al., 2000; Matsumoto et al., 2002).

To predict the effects of global warming on ecosystem dynamics and biogeochemical cycles, we must use an ecosystem model that explicitly represents the differences in plankton groups and nutrients. An ecosystem model, NEMURO (North Pacific Ecosystem Model Used for Regional Oceanography) (Kishi et al., 2007), developed by the model task team of PICES (North Pacific Marine Science Organization), can represent such differences in plankton groups. In this model, phytoplankton and zooplankton, as prognostic variables, are divided into two and three categories, respectively, so that they can accurately represent plankton dynamics. NEMURO successfully simulated the observed interannual variations during 1948–2002, especially the regime shift in the 1970s in the western North Pacific (Aita et al., 2007). This validation for NEMURO confirms that our predictions of changes in ecosystem dynamics and biogeochemical cycles associated with the global warming are realistic.

In order to identify the processes through which global warming affects seasonal and horizontal changes in phytoplankton biomass and in the transition of phytoplankton groups, we conducted present-day and global warming experiments using this model. In this study, we have developed a 3D ecosystem-biogeochemical model extended from NEMURO and applied it to the western North Pacific. As boundary conditions for the global warming experiment, we used the physical environment obtained by a coupled ocean-atmosphere general circulation model (CO-AGCM) developed by CCSR/NIES (Center for Climate System Research, University of Tokyo/National Institute for Environmental Studies).

In the next section, the model is briefly described. In Section 3, we compare results of the present and global warming experiments. We discuss the effects of the global warming on ecosystem dynamics in Section 4 and we summarize in the final section and offer some concluding remarks.

2. Model

As a 3D ecosystem-biogeochemical model for the present-day and global warming experiments, we used the model developed by Hashioka and Yamanaka (2007). We used results in HY as the present-day experiment. In this section, we explain the design of the global warming experiment and show changes in the physical environment obtained from this experiment.

2.1. *Design of the global warming experiment*

In order to generate boundary conditions for the global warming experiment, we used data under the IS92a global warming scenario conducted by CCSR/NIES CO-AGCM (Nozawa et al., 2001), which are contributed to the 3rd report by the Intergovernmental Panel on Climate Change (IPCC, 2001). The IS92a scenario is an intermediate global warming scenario among six of those used in IPCC reports (IPCC, 1996, 2001). The boundary conditions (wind stress, sea surface temperature (SST), fresh water flux and shortwave solar radiation (SSR)) are obtained by adding anomalies to the present-day boundary conditions described in HY. These anomalies were generated using model-data averaged from 2090 to 2100 in the CCSR/NIES global warming experiment. From these data we subtracted the present-day simulation data.

The SST anomaly for the boundary condition of the global warming experiment increases by 2–3 °C in almost all regions, except the Sea of Okhotsk throughout the year, in which the anomaly is almost zero (Fig. 1a). From January to April, the SST anomaly in this region is a large negative value with a negative SSR anomaly (Fig. 1c) due to the increase in clouds. The fresh water flux anomaly is also a large negative value (about $-1.5\,mm\,day^{-1}$) due to the increase in evaporation in the subtropical region and a positive value (about $0.5\,mm\,day^{-1}$) when there is an increase in precipitation in the subarctic region (Fig. 1b).

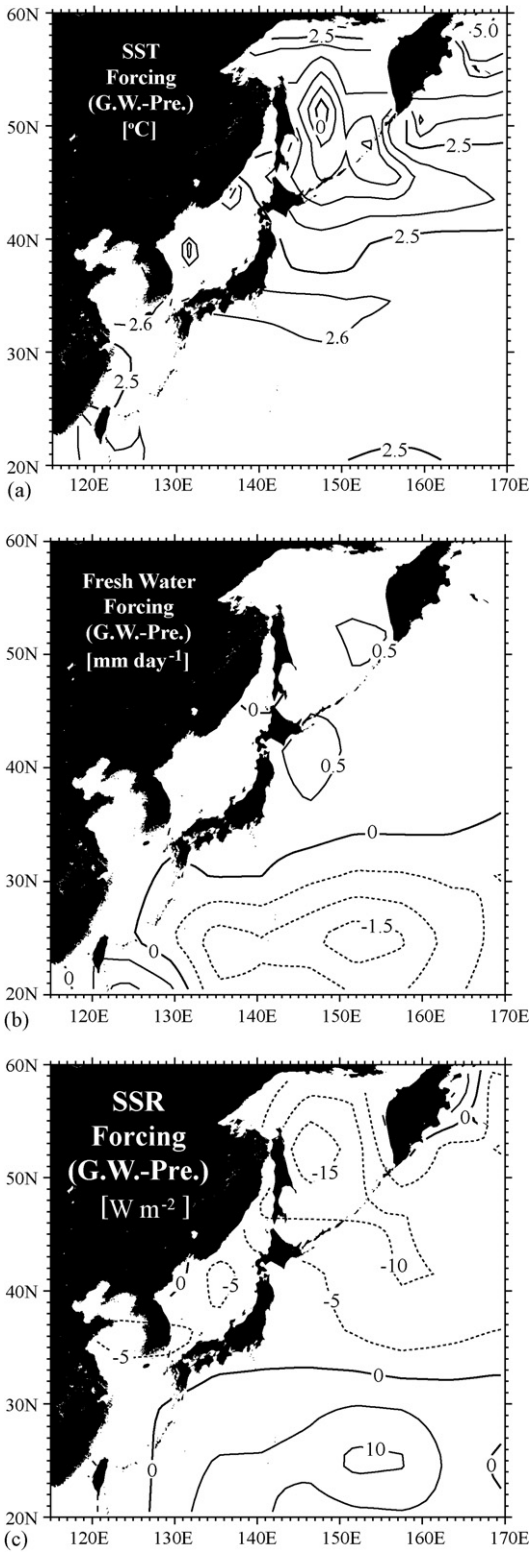

Fig. 1 – Annually averaged anomalies for the boundary conditions of the global warming experiment: (a) sea surface temperature, (b) fresh water flux and (c) short wave solar radiation. Anomalies are calculated by subtracting data averaged from 2090 to 2100 in the CCSR/NIES global warming experiment from those of a present-day experiment (Nozawa et al., 2001).

Nutrient supplies by rivers are assumed to be the same amount in the present-day experiment. Conditions along the eastern and southern boundaries (170–180°E, 10–15°N, respectively) of the model domain for temperature, salinity and nutrients are weakly restored to the climatological monthly mean values of World Ocean Atlas 2001 (WOA01; Conkright et al., 2001) from the surface to the bottom, and are thus somewhat artificial. These regions are not included in the discussions in this paper.

The physical compartment of 3D NEMURO was calculated for 10 years in the global warming experiment without the ecosystem component, starting from the final state of the present-day experiment. Next, the physical compartment coupled with the ecosystem compartment was spun-up for 5 years. As initial conditions for the ecosystem compartment, concentrations of nitrate and silicate are taken from WOA01. In the following discussions, we use results of the last simulated year, which we regard as quasi-steady-state.

2.2. *Changes in physical environment associated with global warming*

Our model reproduced the present-day physical environment reasonably well as discussed in HY. In the global warming scenario, annually averaged SST in the global warming experiment were predicted to increase by 2–3 °C in all regions, except in the Sea of Okhotsk, following the reference temperature associated with the boundary condition (Fig. 2a). Similarly, predicted annually averaged sea surface salinity (SSS) increased by 0.7 psu at the maximum in the subtropical region due to a decrease in fresh water flux and decreased by 0.3 psu in the subarctic region due to an increase in the fresh water flux, except off eastern Hokkaido (Fig. 2b). A salinity front is formed in the Kuroshio extension region, which is the transition region between subarctic and subtropical gyres. The predicted SSS increase off eastern Hokkaido is caused by the northward shift of the salinity front following the separation latitude of the Kuroshio current (Fig. 3). The Kuroshio current, a western boundary current, is driven by wind stress in the entire Pacific Ocean, and the separation latitude is roughly determined by the latitude of wind stress curl equal to zero in the course resolution model. Since the wind stress is strengthened by the global warming, the separation latitude is shifted northward and the maximum Kuroshio current is strengthened from 40 to 50 cm s^{-1}. The seasonal maximum mixed-layer depth (MLD) in the present-day experiment is about 250 m and is located south of the Kuroshio and the Kuroshio extension region near 40°N, whose distribution and maximum depth are consistent with those of observed (Suga et al., 2004). The change in the maximum MLD is large in the subarctic–subtropical transition region where maximum MLD is especially deep. In the global warming experiment, the MLD becomes shallower by 50–100 m along the southern part of Kuroshio current (Fig. 2c) due to the temperature increase in the surface water. Some regions where the predicted MLD becomes shallower than 100 m and deeper than 200 m are located along the Kuroshio extension near 42°N due to the northward shift of the separation latitude of Kuroshio current. In the subtropical region, the MLD is predicted to become

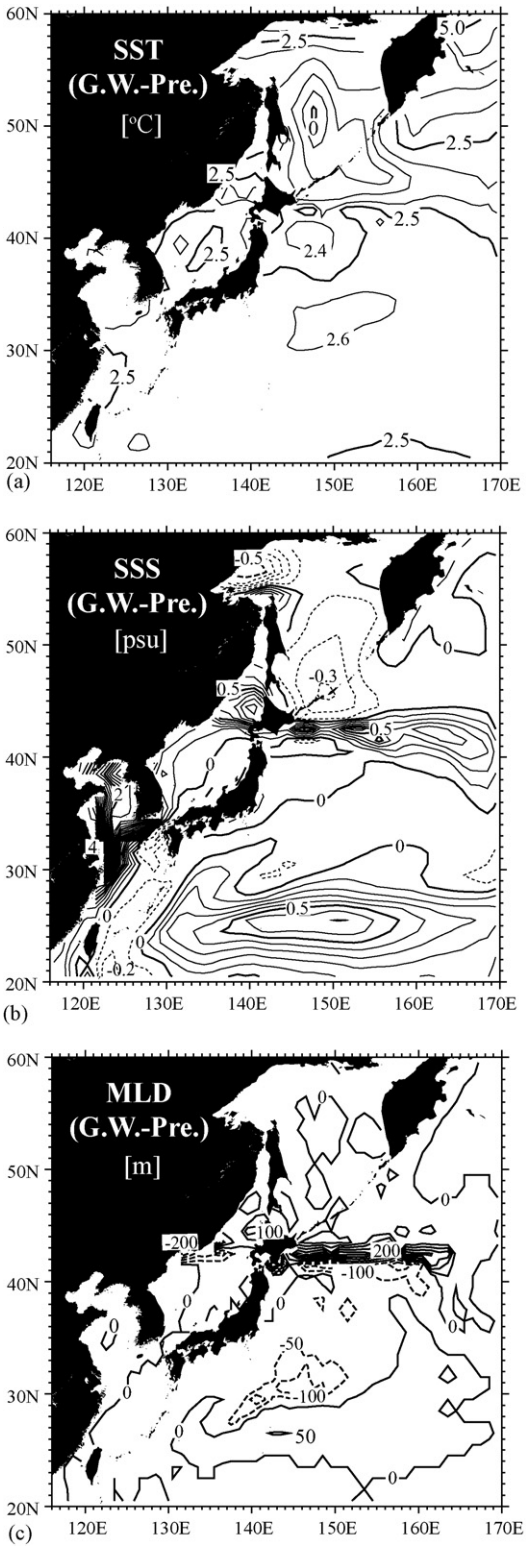

Fig. 2 – Annually averaged changes from the present-day associated with global warming, i.e., the global warming experiment (G.W.) minus the present-day experiment (Pre.), for (a) sea surface temperature, (b) sea surface salinity and (c) maximum winter MLD. Contour intervals are at 0.5 °C for (a), 0.1 psu for (b) and 50 m for (c).

slightly deeper due to the increase in salinity in the surface water.

3. Results

Model results in the present experiment reproduced the observed distributions of nutrients and chlorophyll-*a* concentrations and biomass of diatom as a percentage of total phytoplankton (hereafter, we call this value 'percentage of diatoms'), as discussed in HY. Nutrient concentrations in the surface water are determined by nutrient supplies from the deep water associated with vertical winter mixing and by regeneration rates of nutrients within the surface water. Annually averaged nitrate concentrations at 20 m in the global warming experiment decreases by 1–2 μmol N l^{-1} in the subarctic region and by less than 1 μmol N l^{-1} in the subtropical region (Fig. 4a). Regions of increased and decreased nitrate concentrations are located along the Kuroshio extension near 42°N due to the large change in MLD. The change in the nitrate concentration in the subtropical region is small, but the percentage of concentration change compared to that of the present-day is large. The relatively large change related to the half-saturation constant for nutrient uptake of phytoplankton causes a transition of phytoplankton groups due to the difference in their half-saturation constants.

Annually averaged chlorophyll-*a* concentration in the global warming experiment is predicted to decrease by 0.1–0.3 mg m^{-3} in the subarctic and transition regions and by less than 0.1 mg m^{-3} in the subtropical region, following the decrease in nitrate concentration (Fig. 4b). Note however that chlorophyll-*a* concentration is not only determined by nutrient concentration. Annually averaged percentage of diatoms in the present experiment is 50–60% in the subarctic and less than 30% in the subtropical regions (Fig. 4c). This is consistent with known plankton distributions showing diatoms as the dominant phytoplankton group in the subarctic region and other small phytoplankton as the dominant group in the subtropical region. Since the transition of

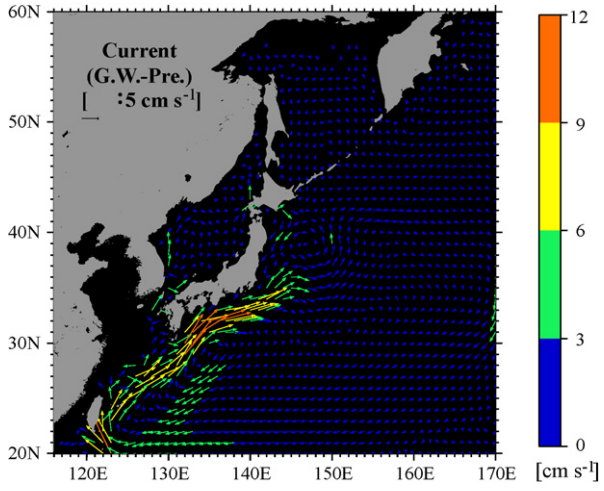

Fig. 3 – Annually averaged changes from the present-day associated with global warming, i.e., the global warming experiment (G.W.) minus the present-day experiment (Pre.), for the flow field at 100 m.

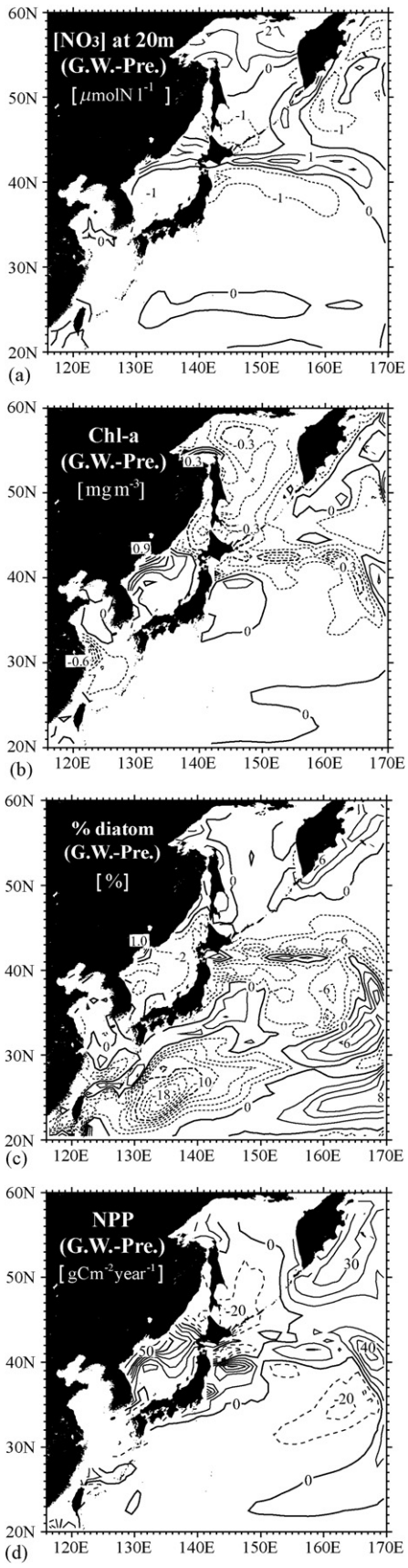

Fig. 4 – Annually averaged changes from the present-day associated with global warming, i.e., the global warming experiment (G.W.) minus the present-day experiment (Pre.), for (a) nitrate concentration at 20 m, (b) chlorophyll-*a* concentration averaged over the upper 10 m, (c) biomass of diatom as percentage of total phytoplankton averaged over surface 20 m and (d) NPP averaged over surface 20 m. The chlorophyll-*a* concentration is converted from nitrogen concentration of phytoplankton using a C:N of 138:16 and a C:chlorophyll-*a* of 1:50. Contour intervals are at 1 μmol N l^{-1} for (a), 0.1 mg cm^{-3} for (b), 2% for (c) and 10 g cm^{-2} $year^{-1}$ for (d).

the dominant phytoplankton group is sensitive to changes in nutrient concentration near the half-saturation constant for nutrient uptake, which is discussed in detail in HY, the change in the percentage of diatoms in the subtropical region associated with the global warming is larger than that in the subarctic region (i.e., 18% decrease at the maximum in the subtropical region and 6% decrease at the maximum in the subarctic region).

The annually averaged net primary production (NPP), calculated as the gross primary production (GPP) minus respiration and extracellular excretion, increases by 20% at the maximum in the subarctic and transition regions except the western side of the Sea of Okhotsk (Fig. 4d). It is interesting that regions of positive NPP anomaly spread out widely, although decreases in nutrient and chlorophyll-*a* concentrations might cause decreases in NPP through a decrease in photosynthetic rate. This is due to favorable temperature conditions associated with the global warming scenario, as discussed in Section 4.1 below. The NPP in the western side of the Sea of Okhotsk decreases with nitrate concentration, as the temperature rise is small. The NPP in the subtropical region, where photosynthesis is not restricted by temperature, increases with nutrient supply. These results are consistent with the decreases in export production and e-ratio (see Section 4.1).

4. Discussion

To understand the change in NPP associated with global warming, we discuss changes in the P/B ratio, a ratio of photosynthetic rate to biomass, e-ratio, a ratio of export to primary productions and export production (Section 4.1). We also discuss changes in seasonal variations of phytoplankton biomass and dominant phytoplankton groups (Section 4.2).

4.1. *Changes in environment for photosynthesis and in export production*

In order to understand how the environment for photosynthesis is changed by global warming, we compared specific photosynthetic rate (P/B ratio; its definition and properties in the present experiment are described in HY) in the present experiment with that in the global warming experiment (Fig. 5a). Annually averaged P/B ratio for total phytoplankton at all latitudes (from 20–50°N) slightly increases. The P/B ratio is affected by nutrient, temperature and light conditions.

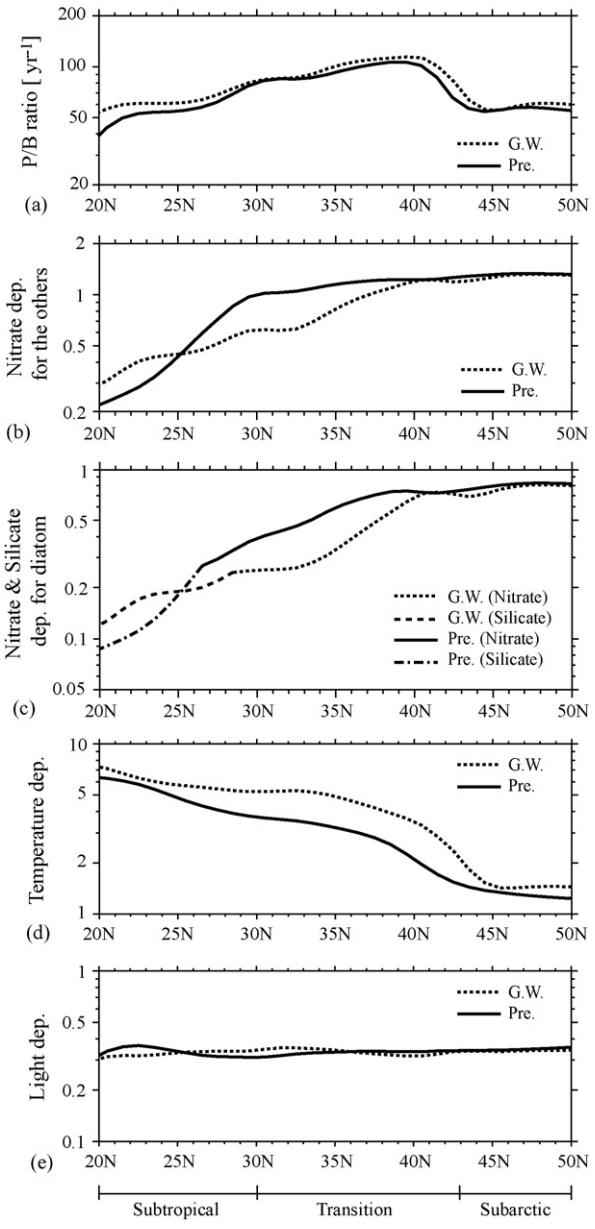

Fig. 5 – (a) Annual P/B ratios for total phytoplankton averaged over surface 100 m and averaged from 150 to 160°E. Annual average dependency of photosynthesis on (b) nitrate for the other small phytoplankton, (c) nitrate and silicate for diatoms, (d) temperature and (e) light averaged over surface 100 m. Dotted lines show result obtained by the global warming experiments and solid lines show results from the present-day experiment. Note that small values in (b) through (e) represent strong limitation. In (c), dotted and solid lines represent nitrate limitations in the global warming and present-day experiments, respectively, and the dash-dotted lines represent silicate limitations for diatoms in the global warming and present-day experiments, respectively. A line representing stronger limitation between nitrate and silicate limitations is only shown in Fig. (c).

Nutrient conditions in all regions, especially in the transition region, except at latitudes lower than 25°N, became worse due to strengthened stratification (Fig. 5b and c). The temperature condition in all regions is predicted to be more favorable, especially in the transition region, since photosynthetic rate increases with temperature (Fig. 5d). The change in light condition is small compared with the others (Fig. 5e). Therefore, the increase in the P/B ratio is caused by the improvement in temperature conditions, although nutrient conditions worsened. In the transition region, although changes in temperature and nutrient conditions are large, they cancel each other out, reducing the changes in the P/B ratios.

Export production is determined by primary production and by the regeneration rate in the surface water. Annually averaged GPP in the present experiment (Fig. 6a), which is integrated over the surface water (upper 100 m), has a maximum in the northern part of the transition region due to the largest P/B ratio (Fig. 5a). The GPP in the global warming experiment increases in almost all regions except in the southern part of the transition region (from 30 to 36°N) compared to in the present experiment. This change in GPP is consistent with those in NPP (Fig. 4d), i.e., GPP minus respiration and extracellular excretion, but the change in NPP is smaller than that

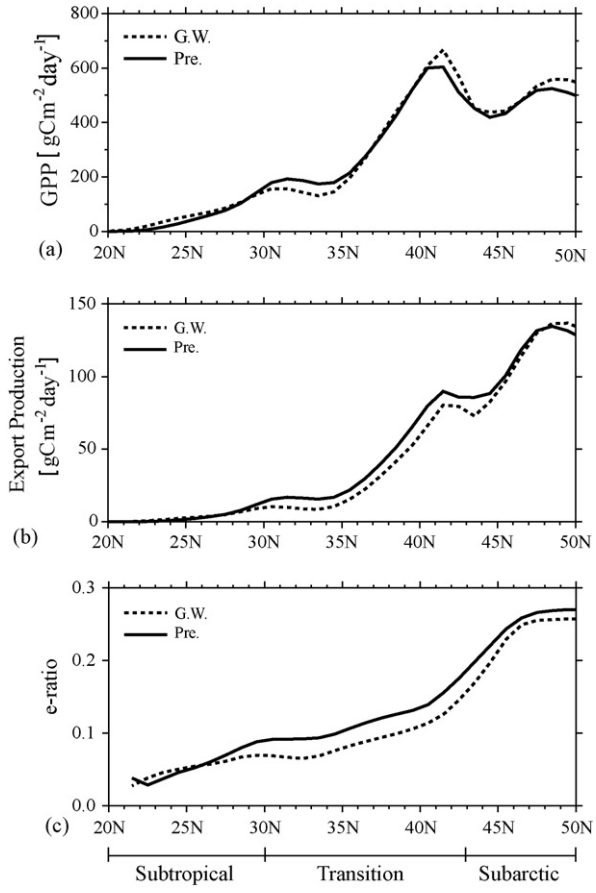

Fig. 6 – Annually averaged (a) gross primary production integrated over the upper 100 m, (b) export production at 100 m and (c) e-ratio, a ratio of export to primary productions. Results are averaged from 150 to 160°E. Dotted and solid lines represent global warming and present-day experiments, respectively.

in GPP, as respiration and extracellular excretion also increase with rising of temperature associated with global warming.

The e-ratio at 100 m depth in the subarctic region in the present-day experiment is higher than those in the other regions (Fig. 6c). The e-ratio in the global warming experiment decreases from that in the present experiment in almost all regions, especially a large decrease in the transition region (decreases by 10–20%), except for the subtropical region (southern part of 26°N). The decrease in e-ratio means that there is an increase in regeneration rate within the surface layers caused mainly by rising temperatures, i.e., almost all processes in the oceanic ecosystem are strongly accelerated with rising temperatures because of their temperature dependence.

The export production at 100 m depth in the subarctic region in the present-day experiment is larger than in other regions because the productivity is higher (Fig. 6b) and the decomposition rate is lower due to lower temperatures, i.e., the e-ratio is high. The export production in the global warming experiment decreases relative to that in the present-day experiment in all regions. The decrease in export production is consistent with the decrease in nutrient supply from deep water to surface water. Therefore, the increases in NPP and GPP are caused by the increase in the P/B ratio, although new production in the surface water decreases. Increases in the regeneration rates of nutrient in the surface water (i.e., decrease in the e-ratio) due to rising of temperature also contribute to the increase in NPP and GPP through (remineralized) nutrient supplies.

4.2. *Changes in seasonal variations of phytoplankton biomass and dominant phytoplankton groups*

We investigated how changes in the oceanic environment associated with global warming affect seasonal variations of phytoplankton biomass and percentage of diatoms at three typical sites (Fig. 7): a Kuroshio extension site (155°E, 40°N), a subarctic site (155°E, 48°N) and a subtropical site (155°E, 28°N). We also investigated which factors related to photosynthesis and grazing control the seasonal variations of phytoplankton biomass (Fig. 8a), using the specific net growth rate of phytoplankton and specific grazing rate by zooplankton, as detailed in HY.

Changes in the biomass and the percentage associated with global warming have common features among the three sites, including: (1) decreases in the annual averaged biomass and percentage, (2) increases in the biomass before the spring bloom, (3) large decreases in the biomass and the percentage at the end of spring bloom, (4) no large change in the biomass and the percentage in summer, among others. That is, it is interesting that the changes do not uniformly occur in all seasons, but occur dramatically at the end of spring bloom and in the fall bloom. As discussed in the previous sections, changes in the MLD, temperature and nutrient concentrations are large in the transition regions. As a result, changes in the biomass and the percentage in the Kuroshio extension site associated with the global warming is the largest among the three sites. Therefore, we will discuss the changes at the Kuroshio extension site as a typical site where the changes are clear. Of course, the following discussions can be applied to the other sites as well.

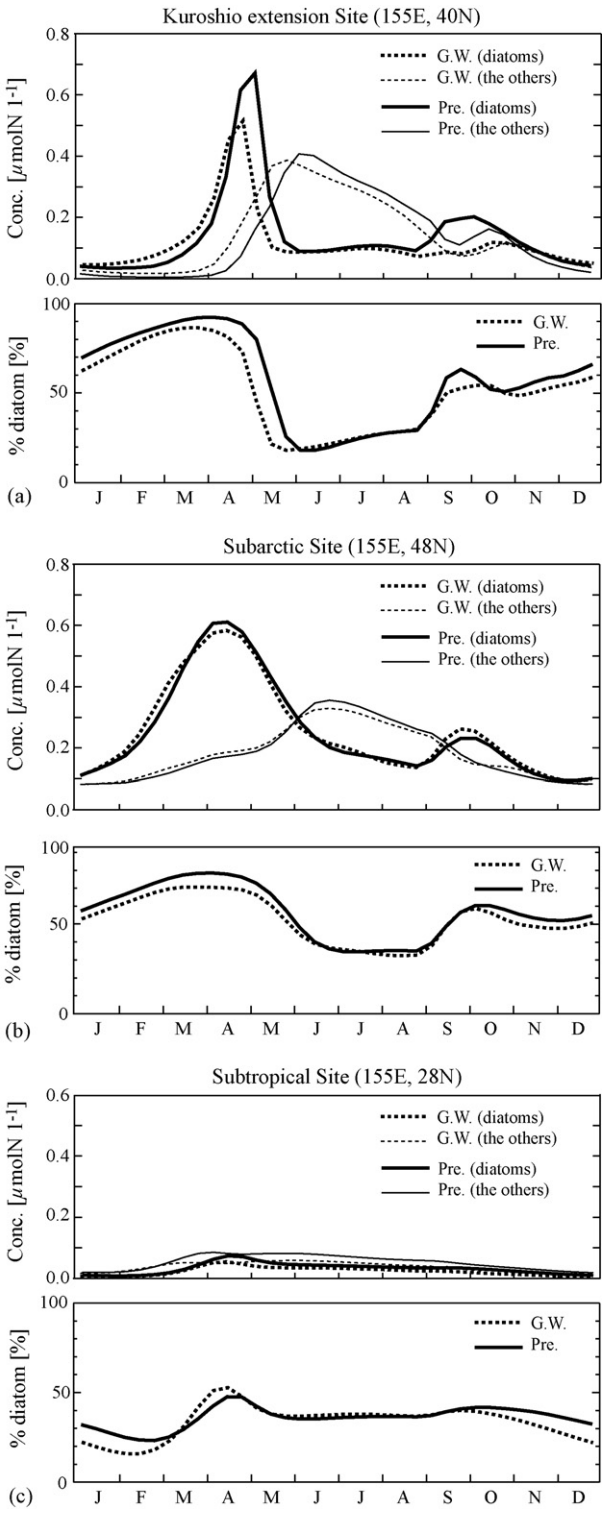

Fig. 7 – Seasonal variations of chlorophyll-*a* concentrations of diatoms (thick line) and other small phytoplankton (thin line) and biomass of diatoms as a percentage of total phytoplankton averaged over the surface 20 m at (a) the Kuroshio extension site (155°E, 40°N), (b) the subarctic site (155°E, 48°N) and (c) the subtropical site (155°E, 28°N). Dotted and solid lines represent the global warming and present-day experiments, respectively.

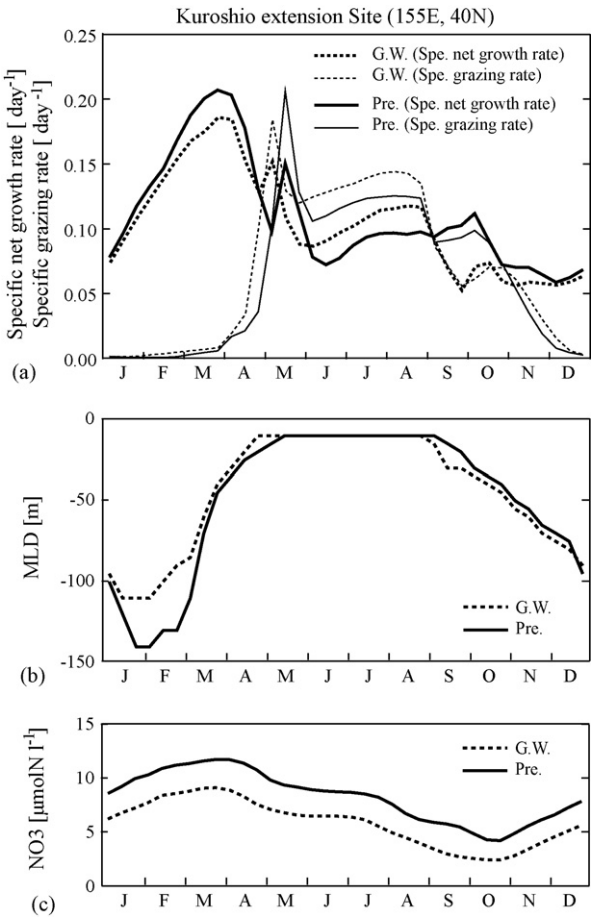

Fig. 8 – Seasonal variations of (a) the specific growth rate of total phytoplankton (thick line) and the specific total zooplankton grazing rate averaged over the surface 20 m (thin line), (b) MLD and (c) the nitrate concentration averaged over the surface 20 m at the Kuroshio extension site (155°E, 40°N). Dotted and solid lines represent the global warming and present-day experiments, respectively.

The concentration of diatoms in the surface water before the diatom spring bloom, from January to March, in both experiments are lowest through the year due to strong dilution caused by the deep winter mixing (Fig. 7a). However the concentration in the global warming experiment is slightly higher than that in the present-day experiment due to weaker dilution caused by increased stratification, i.e., the MLD becomes 50 m shallower in January and February (Fig. 8b). As a result, the onset of the spring bloom in the global warming experiment occurs 1.5 month earlier. The specific net growth rate in the surface waters before the spring bloom in both experiments rapidly increases to the maximum in March, as the temperature and light conditions for photosynthesis are improved by an increase in stratification with high nutrient concentrations (Fig. 8). The rate in the global warming experiment decreases by 15% in March due to lower nutrient concentrations compared with the present-day simulation; and the nitrate concentration decreases by 3 μmol N l^{-1} in March.

The diatom spring bloom in the present experiment at the Kuroshio extension site is terminated by the decrease in the specific net growth rate with nutrient exhaustion for diatoms and by an increase in the specific grazing rate by copepods (not shown), as discussed in HY. The specific grazing rate rises with temperature and is also dependent on both phytoplankton and zooplankton concentrations. The specific grazing rates in the spring bloom in the global warming experiment increase earlier by 1.5 month relative to the present-day experiment and the shift is especially clear in April and May because of higher temperatures and earlier increases in phytoplankton concentration. As a result, the diatom spring bloom in the global warming experiment is terminated early by one half month. Also, the maximum biomass of diatoms in April in the global warming experiment decreases 30% relative to that in the present-day experiment due to the decrease in the specific net growth rate and to the increase in specific grazing rate.

The other small phytoplankton in the global warming experiment also increases one half month earlier than in the present-day experiment. Unlike diatoms, the other small phytoplankton have the same maximum of biomass after the end of diatom spring bloom as that in present-day experiment, since they can adapt to low nutrient conditions due to their small half-saturation constant for nutrient uptake. Therefore, the change in the percentage of diatoms relative to that in the present-day experiment is more noticeable at the end of spring bloom with a decrease of 35%.

Since the present nutrient concentrations and phytoplankton biomass from summer to winter are low compared with those in spring, the predicted changes associated with the global warming scenario are small. The specific net growth and specific grazing rates in summer in the global warming experiment largely increase from that in the present-day experiment, since the rates exponentially increase with the rise of temperature (Fig. 8a). The fall bloom of diatoms at this site in the present experiment is caused by the increase in nutrient supply associated with the development of MLD and by the decrease in grazing pressure by zooplankton. The fall bloom in the global warming experiment does not occur as a consequence of the low nutrient concentrations in autumn, with the result that the percentage of diatoms decreases by 10% from that in present-day experiment.

5. Summary and conclusions

To predict the effects of global warming on ecosystem dynamics and biogeochemical cycles, we developed a 3D ecosystem-biogeochemical model based on NEMURO developed in PICES (Kishi et al., 2007), and applied it to the western North Pacific. Using data sets of observed climatology and simulated fields according to a global warming scenario (CO-AGCM developed by CCSR/NIES, Nozawa et al., 2001) as boundary conditions for our model, we conducted experiments to explore possible effects of global warming on marine ecosystems.

The model results in the present-day experiment reproduced the observed distributions and seasonal variations of nutrient and chlorophyll-*a* concentrations reasonably well (see Hashioka and Yamanaka, 2007). The MLD in the global warming experiment decreases from that in the present experiment, especially in the subarctic–subtropical transition

region. As a result, annually averaged nutrient and phytoplankton concentrations decrease at the end of the 21st century, most markedly in the transition region due to the large change in MLD. The shift from diatoms to other small phytoplankton in the subtropical region is larger than those in the other regions because subtropical nutrient concentrations are close to the half-saturation constant for nutrient uptake of each phytoplankton group, where each has a different value. The P/B ratio for total phytoplankton in the global warming experiment slightly increases from that in the present experiment due to more favorable temperature conditions, although nutrient conditions become worse. The increase in the P/B ratio causes increases in NPP and GPP associated with the global warming. Increases in the regeneration rates (i.e., decrease in the e-ratio) with increases in temperature also contribute to the increase in NPP and GPP through the increase in nutrient supplies, although new and export productions in the surface water decreases.

The changes in seasonal variation of the biomass and percentage in the transition region associated with global warming are the largest in all regions. The diatom spring bloom in the global warming experiment occurs one half month earlier than in the present-day simulation due to strengthened stratification. The maximum biomass in the spring bloom decreases from that in the present-day experiment with decreases in nutrient concentration, i.e., the biomass of diatoms in the transition region decreases by 30%. On the other hand, the biomass of the other small phytoplankton at the maximum after the end of the diatom spring bloom is the same as that in the present experiment because they can adapt to the low nutrient conditions because of their small half-saturation constant. Therefore, the change of the dominant phytoplankton group appears notably at the end of spring bloom, e.g., the percentage of diatoms in the transition region decreases by 35%. Since present nutrient concentrations and phytoplankton biomass from summer to winter are low compared with those in spring, the changes associated with the global warming scenario are small.

The timing of the spring bloom and the subarctic–subtropical transition region (i.e., the Kuroshio–Oyashio transition region) are essential for growth and survival of small pelagic fishes including Japanese sardine and anchovy and Pacific saury (Kasai et al., 1992; Heath et al., 1998; Okazaki et al., 2002). Takahashi (2001) suggested that the abundance of adult anchovy in the waters off northern Japan depend on the growth rate and the duration of early life stages in the Kuroshio–Oyashio transition region during the period when the population size is large. This is because bigger larvae with faster growth rates have a shorter larval stage duration, experience lower mortality, and have a higher probability of surviving to recruitment (Houde, 1987; Anderson, 1988). Our results suggest that the largest changes in phytoplankton biomass and percentage in the transition region associated with global warming, especially during the period of the diatom spring bloom, might significantly decrease the abundance of fish resources in the adult stage.

We investigated effects of the global warming on ecosystem dynamics and biogeochemical cycles at the end of the 21st century. We must investigate the results through the 21st century, as the next step, to understand how changes might occur as a result of global warming, e.g., whether changes are gradual or drastic, such as during a regime shift. Since IS92a is an intermediate scenario of global warming, we should conduct more experiments according to the other scenarios to predict these changes and the upper and lower limits of the effect on global warming. In this study, we demonstrated the effects of global warming on the ecosystem dynamics as a one-way interaction from the climate to the ecosystem. To further discuss their interactions, including feedbacks from the ecosystem to climate, we should develop a climate model (i.e., CO-AGCM) including the ecosystem. It is important to project the impacts to global warming to fishery resources using the model, which can explicitly represent the dynamics of fishery resources. See for example, NEMURO.FISH (Megrey et al., 2007). The global warming experiment in this study was conducted under the assumption that the physiological parameters in NEMURO, which are based on the present ecosystem, will not change due to global warming. However, we would expect their values to change in the future, e.g., in association with shifts of plankton groups from subarctic to subtropical groups. That is, we should estimate the physiological parameters through a greater number of observations and measurements in various environments with seasonal and/or interannual variations in numerous regions and simulate these observed features to predict future ecosystem changes associated with global warming.

Acknowledgements

The authors wish to thank Dr. Hiroyasu Hasumi and Ms. M.N. Aita for offering the CCSR Ocean Component Model (COCO) and for assisting with its use. They would like to thank Dr. Toru Nozawa for providing the data set conducted by CCSR/NIES CO-AGCM. They would also like to thank Drs. Naoki Yoshie and Michio J. Kishi for their helpful comments. They also thank two anonymous reviewers and an editor for their kind comments and thorough proofreading. Thanks are extended to Mr. Takayoshi Ikeda for his proofreading of the English manuscript. One of authors, Taketo Hashioka, was supported by the 21st Century Center of Excellence Program funded by MEXT. This work was partly supported by grants-in-aid 15510001 for scientific research from MEXT.

REFERENCES

Aita, M.N., Yamanaka, Y., Kishi, M.J., 2007. Interdecadal variation of the lower trophic ecosystem in the North Pacific between 1948 and 2002, in a 3-D implementation of the NEMURO model. Ecol. Modell. 202, 81–94.

Anderson, J.T., 1988. A review of size-dependent survival during pre-recruit stages of fishes in relation to recruitment. J. Northwest Atl. Fish. Sci. 8, 55–66.

Archer, D., Maier-Reimer, E., 1994. Effect of deep-sea sedimentary calcite preservation on atmospheric CO_2 concentration. Nature 367, 260–263.

Archer, D., Lea, D., Mahowald, N., 2000. What caused the glacial/interglacial atmospheric pCO_2 cycles? Rev. Geophys. 38, 159–189.

Conkright, M.E., Locarnini, R.A., Garcia, H.E., O'Brien, T.D., Boyer, T.P., Stephens, C., Antonov, J.I., 2001. World Ocean Atlas 2001:

Objective Analyses, Data Statistics, and Figures, CD-ROM Documentation. National Oceanographic Data Center, Silver Spring, p. 17.
Hashioka, T., Yamanaka, Y., 2007. Seasonal and regional variations of phytoplankton groups by top-down and bottom-up controls obtained by a 3-D Ecosystem model. Ecol. Modell. 202, 68–80.
Heath, M.R., Zenitani, H., Watanabe, Y., Kimura, R., Ishida, M., 1998. Modelling the dispersal of larval Japanese sardine, Sardinops melanostictus, by the Kuroshio Current in 1993 and 1994. Fish. Oceanogr. 7, 335–346.
Houde, E.D., 1987. Fish early life dynamics and recruitment variability. Am. Fish. Soc. Symp. 2, 17–29.
IPCC, 1996. Climate Change 1995: The Science of Climate Change. Contribution of Working Group I to the Second Assessment Report of the Intergovernmental Panel on Climate Change, Houghton, J.H., Meira Filho, L.G., Callander, B.A., Harris, N., Kattenberg, A., Maskell, K. (eds.), Cambridge University Press, Cambridge, UK and New York, NY, USA, p. 572.
IPCC, 2001. Climate Change 2001: The Scientific Basis. Contribution of Working Group I to the Third Assessment Report of the Intergovernmental Panel on Climate Change, Houghton, J.T., Ding, Y., Griggs, D.J., Noguer, M., van der Linden, P., Dai, X., Maskell, K., Johnson, C.I. (eds.), Cambridge University Press, U.K., p. 881.
Kasai, A., Kishi, M.J., Sugimoto, T., 1992. Modelling the transport and survival of Japanese sardine larvae in and around the Kuroshio Current. Fish. Oceanogr. 1, 1–10.
Kishi, M.J., Kashiwai, M., Ware, D.M., Megrey, B.A., Eslinger, D.L., Werner, F.E., Aita, M.N., Azumaya, T., Fujii, M., Hashimoto, S., Huang, D., Iizumi, H., Ishida, Y., Kang, S., Kantakov, G.A., Kim, H., Komatsu, K., Navrotsky, V.V., Smith, S.L., Tadokoro, K., Tsuda, A., Yamamura, O., Yamanaka, Y., Yokouchi, K., Yoshie, N., Zhang, J., Zuenko, Y.I., Zvalinsky, V.I., 2007. NEMURO – introduction to a lower trophic level model for the North Pacific marine ecosystem model. Ecol. Modell. 202, 12–25.
Matsumoto, K., Sarmiento, J.L., Brzezinski, M.A., 2002. Silicic acid leakage from the Southern Ocean as a possible mechanism for explaining glacial atmospheric pCO_2. Global Biogeochem. Cycl. 16 (3), 1031.
Megrey, B.A., Rose, K.A., Klumb, R., Hay, D.E., Werner, F.E., Eslinger, D.L., Smith, L., 2007. A bioenergetics-based population dynamics model of Pacific herring (*Clupea harengus pallasii*) coupled to a lower trophic level nutrient-phytoplankton-zooplankton model: Description, calibration and sensitivity analysis. Ecol. Modell. 202, 144–164.
Nozawa, T., Emori, S., Numaguti, A., Tsushima, Y., Takemura, T., Nakajima, T., Abe-Ouchi, A., Kimoto, M., 2001. Projections of Future Climate Change in the 21st Century Simulated by the CCSR/NIES CGCM Under the IPCC SRES Scenarios. Present and Future of Modeling Global Environmental Change: Toward Integrated modeling. Terra Scientific Publishing Company, Tokyo, Japan, pp. 29–48.
Okazaki, Y., Nakata, H., Kimura, S., 2002. Effects of eddies on the distribution and food availability of anchovy larvae in the Kuroshio extension. Mar. Freshw. Res. 53, 403–410.
Suga, T., Motoki, K., Aoki, Y., Macdonald, A.M., 2004. The north Pacific climatology of winter mixed layer and mode waters. J. Phys. Oceanogr. 34 (1), 3–22.
Takahashi, M., 2001. Groth and Development of Larval and Juvenile Japanese Anchovy (*Engraulis japonicus*) and their Implications for Recruitment to Spawning Population. Ph.D. Thesis, University of Tokyo, Tokyo, p. 107 (in Japanese).
Watanabe, Y.W., Ono, T., Wakita, M., Maeda, N., Gamo, T., 2003. Synchronous bidecadal periodic changes of dissolved oxygen, phosphate and temperature between the Japan Sea deep water and the North Pacific intermediate water. Geophys. Res. Lett. 30 (24), 2273.
Watanabe, Y.W., Ishida, H., Nakano, T., Nagai, N., 2005. Spatiotemporal decreases of nutrients and chlorophyll-*a* in surface mixed layer of the western North Pacific from 1971 to 2000. J. Oceanogr. 61 (6), 1011–1016.